

Angle resolved relaxation of spin currents by antiferromagnets in spin valves

D. M. Polishchuk,^{1,2,*} A. Kamra,³ T. I. Polek,² A. Brataas,³ and V. Korenivski¹

¹*Nanostructure Physics, Royal Institute of Technology, 10691 Stockholm, Sweden*

²*Institute of Magnetism, NASU and MESU, 03142 Kyiv, Ukraine*

³*Center for Quantum Spintronics, Department of Physics,
Norwegian University of Science and Technology, NO-7491 Trondheim, Norway*

(Dated: March 3, 2022)

We observe and analyze tunable relaxation of a pure spin current by an antiferromagnet in spin-valves. This is achieved by carefully controlling the angle between a resonantly excited ferromagnetic layer pumping the spin current and the Néel vector of the antiferromagnetic layer. The effect is observed as an angle-dependent spin-pumping contribution to the ferromagnetic resonance linewidth. An interplay between spin-mixing conductance and, often disregarded, longitudinal spin conductance is found to underlie our observations, which is in agreement with a recent prediction for related ferromagnetic spin valves.

Spin polarization of the conduction electrons in metallic ferromagnets enables external control of the electrical properties of magnetic multilayers via the relative magnetization orientation of the ferromagnetic layers comprising the multilayer. The resulting angle-dependent transmission of a spin-polarized current is behind prominent effects such as giant [1, 2] and tunneling [3] magnetoresistance (MR) as well as spin transfer torques [4], which paved the way for rapidly developing spin-electronics [5, 6].

The related angle-dependent dissipation of spin-currents is behind the anisotropic [7, 8] and spin-Hall MR [9–11] observed in heavy-metal/antiferromagnet (HM/AF) bilayers [12, 13]. The key characteristic shared by these two effects is the change in the bilayer’s resistance dependent on whether the polarization of the spin current in the HM is collinear or orthogonal to the axis of preferred spin alignment in the AF (its Néel vector \mathbf{N}). The demonstrated feasibility of controlling spin currents in antiferromagnetic nanostructures indicates a considerable potential of the emerging field of antiferromagnetic spintronics [14–17]. However, an explicit, angle-resolved experimental study of the interaction between a spin current and the Néel vector of an AF, as well as its functional form and physical parameter space, that would underpin the existing strong theoretical effort [18–20] is still pending.

Ferromagnetic resonance (FMR) driven spin pumping is a unique tool for analyzing spin relaxation in F/N/F_{st} [21–25] and F/N/AF [26–29] spin valves. The ferromagnetic layer F is the source as well as the probe of a pure spin-current pumped into the nonmagnetic spacer N and static ferromagnetic F_{st} or AF layers. Since there is negligible spin dissipation in the typically nm-thin spacer N, spin pumping probes the spin relaxation due to the static F_{st} or AF layers measured via the back-flow spin-current contribution to the FMR linewidth of F. If the spin absorption by the static layer is anisotropic, the spin-pumping contribution is manifested as an angle-dependent modulation of the FMR linewidth. Indeed,

anisotropic absorption of pure spin currents was reported for F/N/F_{st} [21, 25] but could not be attributed to non-collinearity between the spin-current polarization and magnetization. In Ref. 21, it was attributed to the angle dependence of dynamic exchange, whereas in Ref. 25, it was explained in terms of an angular dependence of the total Gilbert damping in F_{st}. To the best of our knowledge, the anisotropy of spin relaxation studied by controllably varying the angle between the spin-current polarization (set by F) and the magnetic axis of F_{st} or AF has not been demonstrated in magnetic multilayers. The main difficulty in achieving a reliable control of the noncollinear alignment in such spin valve structures lies in the presence of a kOe-range external magnetic field required in a typical FMR experiment, which often fully aligns the studied multilayer magnetically.

In this Letter, we demonstrate controllable magnetic damping in a F layer via ϕ -dependent interaction of the emitted spin pumping current with the Néel vector of an AF layer in a F/N/AF/F_p type spin-valve, where ϕ is the angle between the equilibrium magnetization in F and the AF Néel vector. Carrying out detailed ϕ -dependent, variable-temperature measurements of the FMR-driven, spin-pumping-mediated magnetization damping, we observe a pronounced maximum when the magnetization of F is orthogonal to the AF Néel vector. Our results are well described by a theoretical model analogous to that for ferromagnetic spin valves [30] and indicate the dominance of *longitudinal* over spin-mixing conductance in spin relaxation by the AF layer. This consistency with the recent prediction [30] highlights the importance of longitudinal spin transport in magnetic multilayers and establishes an important pathway towards achieving in-situ damping tunability.

Spin pumping experiment. Spin pumping is an emission of spin angular momentum ($\mathbf{I}_{\sigma}^{\text{pump}}$) by a resonantly precessing ferromagnet (F) into an adjacent nonmagnetic spacer N [31]. In this sense, spin pumping is a reciprocal effect to a spin-transfer torque [32]. $\mathbf{I}_{\sigma}^{\text{pump}}$ carries spin away from F, which increases the magnetization damp-

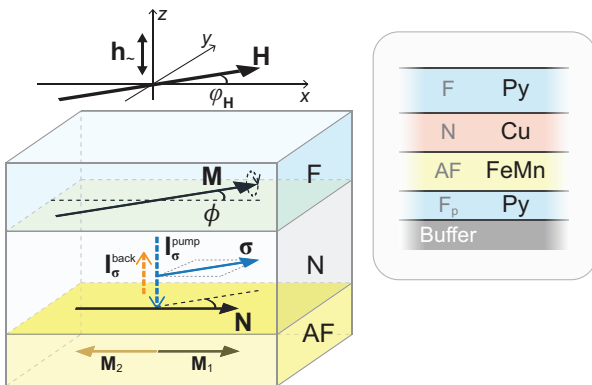


FIG. 1. Schematic of the studied multilayer and the FMR measurement configuration when external magnetic field \mathbf{H} is applied in the film plane xy . The equilibrium axis of resonating magnetization \mathbf{M} in F follows the external field \mathbf{H} , whereas the AF vector \mathbf{N} is fixed in the xy plane (using e.g. a ferromagnetic seed layer, F_p ; inset). Vector \mathbf{N} forms angle ϕ with polarization σ of spin-pumped current $\mathbf{I}_\sigma^{\text{pump}}$.

ing in F, usually detected as a broadening of the F-layer’s FMR linewidth [33, 34]. Considering the F/N/AF trilayer used in this work, and taking spin relaxation in N to be negligible, a fraction of the spin-pumping current is reflected at the N/AF interface and returns back to F. The spin-pumping contribution to the FMR linewidth is proportional to the difference between $\mathbf{I}_\sigma^{\text{pump}}$ and the back-flow spin current $\mathbf{I}_\sigma^{\text{back}}$ (Fig. 1) [32]. A change in the relative orientation between the spin-current polarization σ and the AF’s Néel vector should affect $\mathbf{I}_\sigma^{\text{back}}$ thereby modulating the FMR-linewidth of F.

The F/N/AF trilayer under “in-plane” FMR, illustrated in Fig. 1, has the equilibrium orientation of the resonating magnetization in magnetically soft F (\mathbf{M}) aligned with the external magnetic field (≈ 1 kOe) applied at angle $\varphi_{\mathbf{H}}$. At the same time, the Néel vector \mathbf{N} of AF is essentially insensitive to this relatively weak field and remains directionally fixed, provided it is suitably set in fabrication (as detailed below). This spin valve structure allows to control the angle ϕ between the F layer magnetization and the AF layer Néel vector enabling us to extract the ϕ -dependence of the spin-pumping contribution to the FMR linewidth.

A macroscopic magnetic anisotropy in AF – the key AF property for this study – can be induced by deposition in a static magnetic field and/or post-fabrication magnetic annealing [35]. The other effective approach is to deposit a thin AF layer onto a saturated ferromagnetic seed layer (F_p), which induces a strong exchange bias in the AF/ F_p bilayer. The latter results in a pronounced unidirectional magnetic anisotropy in F_p as well as a magnetic axis in AF. We have fabricated a series of multilayers, where antiferromagnetic FeMn is grown on either a ferromagnetic (Py) or nonmagnetic (Ta) seed layer. Here, FeMn and Py denote $\text{Fe}_{50}\text{Mn}_{50}$ and $\text{Fe}_{20}\text{Ni}_{80}$ (permalloy) alloys. The

thickness of the FeMn layer of 7 nm was found to be optimal as regards to a strong directional exchange bias throughout the FeMn/Py bilayer with a high blocking temperature ($T_b \approx 420$ K) [35, 36]. The opposite surface of the FeMn layer, acting as the spin-current reflector or sink, is interfaced with the free, soft Py layer via a nonmagnetic Cu spacer. The thickness of the Cu layer (6 nm) was chosen much smaller than the spin diffusion length in Cu ($\lambda_s > 100$ nm at room temperature [37]) to ensure negligible spin dissipation in N.

FMR measurements were carried out at a constant frequency of 9.88 GHz while sweeping an external magnetic field \mathbf{H} applied in the film plane. The obtained spectra exhibit a strong resonance line from the free Py layer, the position of which (the resonance field) reveals a very weak uniaxial magnetic anisotropy in the film plane [Figs. 2(a) and (b)]. The FMR spectra for the structures with the FeMn/Py bilayer exhibit an additional weakly-intensive resonance line, which we attribute to the seed Py layer and use as an independent probe of the magnetic directionality of AF. This line exhibits a very pronounced unidirectional anisotropy, indicating a strong exchange bias in the FeMn/Py bilayer [35].

Angle-dependent FMR linewidth. The FMR linewidth of the free Py layer ΔH as well as the resonance field H_r were obtained by fitting the spectra with a Dysonian [38]. ΔH versus $\varphi_{\mathbf{H}}$ for the samples with the magnetic and nonmagnetic seed layers differ significantly in the magnitude of the variation as well as its angular profile [Fig. 2(c)]. On the other hand, the respective resonance fields $H_r(\varphi_{\mathbf{H}})$ show the same behavior [Fig. 2(b)], indicating that the saturation magnetization and the magnetic anisotropy of the free layer are largely unaffected by the seed layer. The observed difference in the magnetic damping (ΔH) for the two structures must therefore be attributed to a difference in the magnetic state of their respective FeMn layers. The essentially isotropic behavior of ΔH for the case of FeMn/Ta indicates that the FeMn layer exhibits no macroscopic magnetic axis (in fact, by design) as antiferromagnetic domains formed on non-magnetic Ta are likely to orient randomly. In contrast, the pronounced anisotropy of ΔH for the structure with the FeMn/Py bottom magnetic layer is evidence for a well-defined macroscopic magnetic anisotropy in the FeMn layer, the conclusion additionally and independently supported by the observed pronounced unidirectional anisotropy in the seed-Py layer [39]. In what follows, we focus on this key result of anisotropic spin relaxation in the FeMn/Py-based structure.

The multilayers with FeMn/Py exhibit a thermally-induced transformation of the ΔH -vs- $\varphi_{\mathbf{H}}$ profile. The maximum in $\Delta H(\varphi_{\mathbf{H}})$ observed at room temperature at $\varphi_{\mathbf{H}} \approx \pm 90^\circ$ shifts to larger angles with decreasing temperature [Fig. 3(a)]. At the same time, there are no temperature-induced changes in the angle profiles of

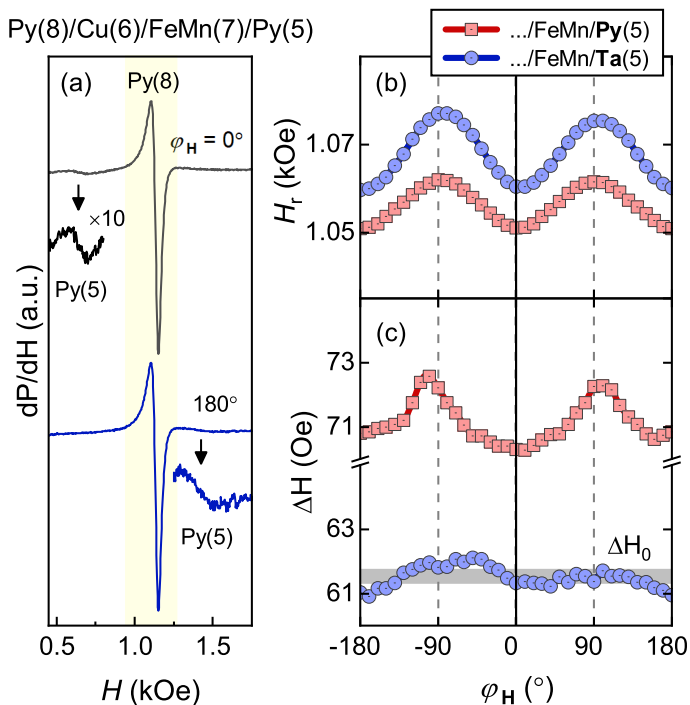


FIG. 2. (a) In-plane FMR spectra measured along (0°) and opposite (180°) to the exchange-pinning direction set by the seed Py(5) layer. (b), (c) Angular dependence of the resonance field (H_r) and the linewidth (ΔH) for the free Py(8) layer for the structures where the antiferromagnetic FeMn layer was grown on nonmagnetic Ta(5) or ferromagnetic Py(5). The data were measured at 280 K.

the resonance field, except the offset in the magnitude of H_r due to the temperature variation in the saturation magnetization of the Py layer [39]. This implies that the observed changes in ΔH -vs- φ_H with temperature are caused by factors external to the free layer – in our case the spin-pumping-mediated effect of the AF on ΔH – rather than by any changes in the intrinsic magnetic properties of the free layer. Importantly, the changes in the angular profiles of Fig. 3(a) are associated with a temperature dependence of the AF layer pinning by the seed underlayer. This is strongly supported by the corresponding ΔH -vs- φ_H for the FeMn/Ta-based structures (without macroscopic magnetic axis), which remain largely isotropic at all temperatures [39].

Spin-pumping contribution. We explain the observed angle-dependence of the FMR linewidth as due to the spin-pumping contribution to the magnetization dynamics of the free layer. We extend the phenomenology of the spin-pumping effect [31, 32] to a non-collinear ferromagnetic-nonmagnetic-antiferromagnetic (F/N/AF) trilayer system. The magnetization dynamics of F is described in terms of the spin conductivities of the F/N and N/AF interfaces for an arbitrary mutual orientation of the respective magnetic order parameters

– magnetization \mathbf{M} and Néel vector \mathbf{N} .

The anisotropic ΔH -vs- φ_H profile, shown in Fig. 2(c), exhibits maxima close to $\varphi_H = \pm 90^\circ$, which can be qualitatively explained as follows. The precessing F pumps spins into the adjacent spacer layer, a fraction of which is subsequently absorbed by AF. The absorbed spin current manifests as additional damping in F. However, only the component of spin current that is orthogonal to the equilibrium F magnetization determines the damping in it. This component is best absorbed when the F magnetization and the AF Néel vector are mutually orthogonal, provided that AF absorbs and dissipates the longitudinal component stronger than the transverse component of the spin current.

In the general case, the spin-pumping contribution to the integral FMR linewidth can be quantitatively expressed in terms of the spin conductances of the F/N and N/AF interfaces [30]. The other contributions, such as the intrinsic Gilbert damping and inhomogeneous terms, have a much weaker dependence on the in-plane angle and add up in the total $\Delta H(\varphi_H)$ to a constant $\Delta H_{\text{int}} \approx \text{const}$ [40]. The case of a noncollinear mutual alignment of \mathbf{M} and \mathbf{N} can be treated in a manner analogous to Ref. 30. The full FMR linewidth becomes

$$\Delta \tilde{H} = \Delta \tilde{H}_0 + 0.5 \frac{\tilde{g}_r \tilde{g}_l}{(\tilde{g}_r \tilde{g}_l + \tilde{g}_r) + (\tilde{g}_l - \tilde{g}_r) \cos^2 \phi}, \quad (1)$$

where $\Delta \tilde{H} = \Delta H \cdot (4\pi MV)/(g_r^* \cdot \hbar \omega)$, ω – the frequency of the applied microwave field, V – the film volume; $\tilde{g}_{l,r} = g_{l,r}/g_r^*$, where the longitudinal spin conductance (g_l) and the real part of the spin-mixing conductance (g_r) characterise the N/AF subsystem, whereas g_r^* relates to the F/N interface. The second term in (1) is the angle-dependent spin-pumping contribution, a function of angle ϕ between \mathbf{M} and \mathbf{N} . $\Delta \tilde{H}_0$, in turn, consists of $\Delta \tilde{H}_{\text{int}}$ and the *angle-independent* spin-pumping contribution: $\Delta \tilde{H}_0 = \Delta \tilde{H}_{\text{int}} + 0.5 \tilde{g}_r / (1 + \tilde{g}_r)$.

Equation (1) can be used for fitting the experimental ΔH -vs- φ_H data. Subtracting the *angle-independent* background ΔH_0 from the total ΔH allows one to fit the data using only the second, angle-dependent term in (1). In this respect, and based on the detailed discussion above [Figure 2(c) and related text], the most appropriate is to take as ΔH_0 the linewidth for the FeMn/Ta-based structure, in fact, specifically designed for this calibration. Figure 3(a) shows the result, which agrees well with the experiment.

Effect of temperature. With changing temperature, the anisotropic spin relaxation undergoes a transformation of its angular form [Fig. 3(a)], which can be explained by the temperature-dependent properties of the exchange-pinned AF/F_p bilayer. The stronger interface exchange-pinning at lower temperatures results in a stronger torque on the AF, such that \mathbf{M} and \mathbf{N} become orthogonal at different angles of the applied in-plane field

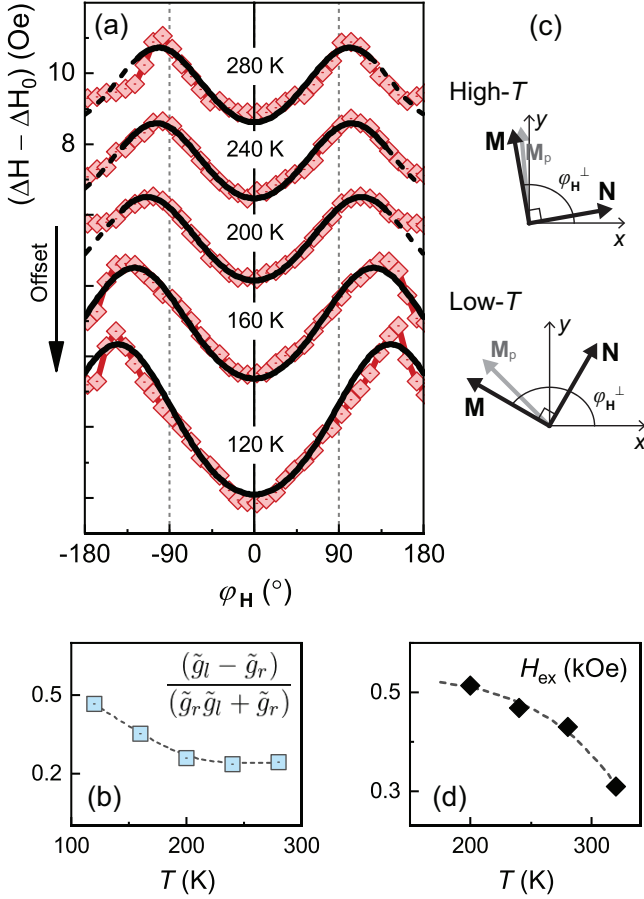


FIG. 3. (a) Angle-dependent spin-pumping contribution ($\Delta H - \Delta H_0$) versus φ_H , obtained from the measured FMR linewidth by subtracting the predominantly isotropic linewidth for the control sample (FeMn/Ta based) at each given temperature. Solid lines are the fits to theory [Eq. (1)]. (b) Extracted from the fitting in (a), the temperature dependence of the spin-relaxation asymmetry parameter. (c) Illustration of the rotating torque on the AF with Néel vector \mathbf{N} by the exchange-coupled Py(5) layer of magnetization \mathbf{M}_p , for two characteristic temperatures. (d) FeMn/Py exchange-pinning field H_{ex} vs temperature, extracted from $H_r(T)$ for Py(5) [Fig. 2(a)].

(of fixed magnitude $H = H_r^F = 1.03\text{--}1.08$ kOe) for different temperatures, as detailed below.

With decreasing temperature, the maximum in ΔH shifts from $\varphi_H \approx \pm 90^\circ$ to larger angles [Fig. 3(a)], which can be explained by a deviation of vector \mathbf{N} (tilt angle φ_N) from its easy (exchange-pinning) direction, so the 90° -rotation of \mathbf{M} with respect to \mathbf{N} occurs at a larger φ_H [field angle measured from the exchange-pinning direction, as illustrated in Figs. 3(c)]. This tilt of \mathbf{N} , increasing at low temperatures for a given field-torque (acting via F_p), is due to the well-known strengthening of the exchange coupling between AF and F_p (increasing from about AF's T_N toward low temperature). The magneti-

zation \mathbf{M}_p of F_p follows the direction of the applied magnetic field \mathbf{H} (the applied 1 kOe exceeds the exchange-pinning field at all temperatures) and, via the exchange at the interface, torques \mathbf{N} off the initial equilibrium orientation ($\varphi_N = 0$). This tilting is quantitatively described by a competition between the exchange bias in the AF/ F_p bilayer (J_{ex}) and the Zeeman energy of F_p (J_Z), as detailed in [39]. With changing temperature, J_Z varies slowly since the Curie point of F_p is much higher than the experimental temperature range, whereas J_{ex} has a pronounced temperature dependence shown by the extracted exchange field $H_{ex}(\sim J_{ex})$ vs T in Fig. 3(d): $H_{ex} \approx 0.5$ kOe vanishes toward the Neel point of the AF (more precisely the blocking point, $T_b \approx T_N$ [35]).

Equation (1) fits the measured data very well for all temperatures [solid lines in Fig. 3(a)], when modified according to the discussion above, such that angle ϕ between \mathbf{M} and \mathbf{N} is scaled by a temperature-dependent parameter reflecting the tilt of the AF, $\phi = (\varphi_H - \varphi_N) = a\varphi_H$ ($a \leq 1$). Our simulations show [39], that the AF tilt angle φ_N is linear in φ_H in the angle interval slightly wider than that between the two maxima in $\Delta H(\varphi_H)$. The parts of the calculated curves outside this fitting interval are dashed in Fig. 3(a). The final result of the analysis is the parameter representing the anisotropic magnetization damping, which is proportional to the difference $(g_l - g_r)$ [Fig. 3(b)] and shows how the observed angle-dependent FMR linewidth directly stems from the spin-conductance asymmetry of the N/AF interface.

Discussion and Conclusion. The result of the above analysis is a finite and positive $(g_l - g_r)$ [Fig. 3(b)], which means that the spin reflection at the N/AF interface is larger when the spin-current polarization $\boldsymbol{\sigma}$ is collinear with the AF's magnetic axis (\mathbf{x}) and smaller for orthogonal $\boldsymbol{\sigma}$ and \mathbf{x} . In arriving at this conclusion, we have assumed that the exchange biasing tends to align the Néel vector of the AF with the seed layer's magnetization. This assumption is supported by the widely accepted *uncompensated-spin* model of exchange bias [41, 42] describing the effect in similar metallic AF/ F_p bilayers [43]. Therefore, our experiment demonstrates that g_l exceeds g_r in the considered metallic AFs, which is consistent with the strong spin relaxation observed in such AFs [26, 27], and is in contrast to the typical assumption, $g_l \ll g_r$, in literature [32, 44, 45].

Furthermore, the shown sensitivity of the magnetization damping in the resonating F layer to the presence of an induced magnetic axis in the static AF layer is an example of how spin-pumping can be used for probing the changes in the spin configuration of AFs subjected to external stimuli (thermal and/or magnetic). Finally, the reported angular modulation of the FMR linewidth is experimental demonstration of an in-situ, spin-pumping-mediated control of magnetization damping in magnetic multilayers predicted recently [30].

Support from the Swedish Research Council (VR

Grant No. 2018-03526), the Swedish Stiftelse Olle Engkvist Byggmästare, and the Research Council of Norway through its Centers of Excellence funding scheme, Project No. 262633, QuSpin, are gratefully acknowledged.

* dpol@kth.se.

- [1] M. N. Baibich, J. M. Broto, A. Fert, F. Nguyen Van Dau, F. Petroff, P. Etienne, G. Creuzet, A. Friederich, and J. Chazelas, “Giant magnetoresistance of (001)Fe/(001)Cr magnetic superlattices,” *Physical Review Letters* **61**, 2472–2475 (1988).
- [2] G. Binasch, P. Grünberg, F. Saurenbach, and W. Zinn, “Enhanced magnetoresistance in layered magnetic structures with antiferromagnetic interlayer exchange,” *Physical Review B* **39**, 4828–4830 (1989).
- [3] J. S. Moodera, Lisa R. Kinder, Terrilyn M. Wong, and R. Meservey, “Large magnetoresistance at room temperature in ferromagnetic thin film tunnel junctions,” *Physical Review Letters* **74**, 3273–3276 (1995).
- [4] J.C. Slonczewski, “Current-driven excitation of magnetic multilayers,” *Journal of Magnetism and Magnetic Materials* **159**, L1–L7 (1996).
- [5] Igor Žutić, Jaroslav Fabian, and S. Das Sarma, “Spintronics: Fundamentals and applications,” *Reviews of Modern Physics* **76**, 323–410 (2004).
- [6] S. Maekawa, S. O. Valenzuela, E. Saitoh, and T. Kimura, eds., *Spin Current*, 2nd ed. (Oxford University Press, 2017).
- [7] B. G. Park, J. Wunderlich, X. Martí, V. Holý, Y. Kurosaki, M. Yamada, H. Yamamoto, A. Nishide, J. Hayakawa, H. Takahashi, A. B. Shick, and T. Jungwirth, “A spin-valve-like magnetoresistance of an antiferromagnet-based tunnel junction,” *Nature Materials* **10**, 347–351 (2011).
- [8] X. Marti, I. Fina, C. Frontera, Jian Liu, P. Wadley, Q. He, R. J. Paull, J. D. Clarkson, J. Kudrnovský, I. Turek, J. Kuneš, D. Yi, J-H. Chu, C. T. Nelson, L. You, E. Arenholz, S. Salahuddin, J. Fontcuberta, T. Jungwirth, and R. Ramesh, “Room-temperature antiferromagnetic memory resistor,” *Nature Materials* **13**, 367–374 (2014).
- [9] S. Y. Huang, X. Fan, D. Qu, Y. P. Chen, W. G. Wang, J. Wu, T. Y. Chen, J. Q. Xiao, and C. L. Chien, “Transport magnetic proximity effects in platinum,” *Physical Review Letters* **109**, 107204 (2012).
- [10] H. Nakayama, M. Althammer, Y.-T. Chen, K. Uchida, Y. Kajiwara, D. Kikuchi, T. Ohtani, S. Geprgs, M. Opel, S. Takahashi, R. Gross, G. E. W. Bauer, S. T. B. Goennenwein, and E. Saitoh, “Spin hall magnetoresistance induced by a nonequilibrium proximity effect,” *Physical Review Letters* **110**, 206601 (2013).
- [11] Yan-Ting Chen, Saburo Takahashi, Hiroyasu Nakayama, Matthias Althammer, Sebastian T B Goennenwein, Eiji Saitoh, and Gerrit E W Bauer, “Theory of spin hall magnetoresistance (SMR) and related phenomena,” *Journal of Physics: Condensed Matter* **28**, 103004 (2016).
- [12] J. H. Han, C. Song, F. Li, Y. Y. Wang, G. Y. Wang, Q. H. Yang, and F. Pan, “Antiferromagnet-controlled spin current transport in SrMnO₃/pthybrids,” *Physical Review B* **90**, 144431 (2014).
- [13] Geert R. Hoogeboom, Aisha Aqeel, Timo Kuschel, Thomas T. M. Palstra, and Bart J. van Wees, “Negative spin hall magnetoresistance of pt on the bulk easy-plane antiferromagnet NiO,” *Applied Physics Letters* **111**, 052409 (2017).
- [14] Takahiro Moriyama, Noriko Matsuzaki, Kab-Jin Kim, Ippei Suzuki, Tomoyasu Taniyama, and Teruo Ono, “Sequential write-read operations in FeRh antiferromagnetic memory,” *Applied Physics Letters* **107**, 122403 (2015).
- [15] P. Wadley, B. Howells, J. elezny, C. Andrews, V. Hills, R. P. Campion, V. Novak, K. Olejnik, F. Maccherozzi, S. S. Dhesi, S. Y. Martin, T. Wagner, J. Wunderlich, F. Freimuth, Y. Mokrousov, J. Kune, J. S. Chauhan, M. J. Grzybowski, A. W. Rushforth, K. W. Edmonds, B. L. Gallagher, and T. Jungwirth, “Electrical switching of an antiferromagnet,” *Science* **351**, 587–590 (2016).
- [16] T. Jungwirth, X. Marti, P. Wadley, and J. Wunderlich, “Antiferromagnetic spintronics,” *Nature Nanotechnology* **11**, 231–241 (2016).
- [17] V. Baltz, A. Manchon, M. Tsoi, T. Moriyama, T. Ono, and Y. Tserkovnyak, “Antiferromagnetic spintronics,” *Reviews of Modern Physics* **90**, 015005 (2018).
- [18] A. S. Núñez, R. A. Duine, Paul Haney, and A. H. MacDonald, “Theory of spin torques and giant magnetoresistance in antiferromagnetic metals,” *Physical Review B* **73**, 214426 (2006).
- [19] Helen V. Gomonay and Vadim M. Loktev, “Spin transfer and current-induced switching in antiferromagnets,” *Physical Review B* **81**, 144427 (2010).
- [20] O. Gomonay, V. Baltz, A. Brataas, and Y. Tserkovnyak, “Antiferromagnetic spin textures and dynamics,” *Nature Physics* **14**, 213–216 (2018).
- [21] Bret Heinrich, Yaroslav Tserkovnyak, Georg Woltersdorf, Arne Brataas, Radovan Urban, and Gerrit E. W. Bauer, “Dynamic exchange coupling in magnetic bilayers,” *Physical Review Letters* **90**, 187601 (2003).
- [22] Tomohiro Taniguchi, Satoshi Yakata, Hiroshi Imamura, and Yasuo Ando, “Determination of penetration depth of transverse spin current in ferromagnetic metals by spin pumping,” *Applied Physics Express* **1**, 031302 (2008).
- [23] A. Ghosh, S. Auffret, U. Ebels, and W. E. Bailey, “Penetration depth of transverse spin current in ultrathin ferromagnets,” *Physical Review Letters* **109**, 127202 (2012).
- [24] M. K. Marcham, L. R. Sheldford, S. A. Cavill, P. S. Keatley, W. Yu, P. Shafer, A. Neudert, J. R. Childress, J. A. Katine, E. Arenholz, N. D. Telling, G. van der Laan, and R. J. Hicken, “Phase-resolved x-ray ferromagnetic resonance measurements of spin pumping in spin valve structures,” *Physical Review B* **87**, 180403(R) (2013).
- [25] A. A. Baker, A. I. Figueroa, C. J. Love, S. A. Cavill, T. Hesjedal, and G. van der Laan, “Anisotropic absorption of pure spin currents,” *Physical Review Letters* **116**, 047201 (2016).
- [26] P. Merodio, A. Ghosh, C. Lemonias, E. Gautier, U. Ebels, M. Chshiev, H. Béa, V. Baltz, and W. E. Bailey, “Penetration depth and absorption mechanisms of spin currents in Ir₂₀Mn₈₀ and Fe₅₀Mn₅₀ polycrystalline films by ferromagnetic resonance and spin pumping,” *Applied Physics Letters* **104**, 032406 (2014).
- [27] L. Frangou, S. Oyarzún, S. Auffret, L. Vila, S. Gambarelli, and V. Baltz, “Enhanced spin pumping efficiency in antiferromagnetic IrMn thin films around the magnetic phase transition,”

- Physical Review Letters* **116**, 077203 (2016).
- [28] Zhiyong Qiu, Jia Li, Dazhi Hou, Elke Arenholz, Alpha T. N'Diaye, Ali Tan, Ken ichi Uchida, Koji Sato, Satoshi Okamoto, Yaroslav Tserkovnyak, Z. Q. Qiu, and Eiji Saitoh, "Spin-current probe for phase transition in an insulator," *Nature Communications* **7**, 12670 (2016).
- [29] Takahiro Moriyama, Michinari Kamiya, Kent Oda, Kensho Tanaka, Kab-Jin Kim, and Teruo Ono, "Magnetic moment orientation-dependent spin dissipation in antiferromagnets," *Physical Review Letters* **119**, 267204 (2017).
- [30] Akashdeep Kamra, Dmytro M. Polishchuk, Vladislav Korenivski, and Arne Brataas, "Anisotropic and controllable gilbert-bloch dissipation in spin valves," *Physical Review Letters* **122**, 147201 (2019).
- [31] Yaroslav Tserkovnyak, Arne Brataas, and Gerrit E. W. Bauer, "Enhanced gilbert damping in thin ferromagnetic films," *Physical Review Letters* **88**, 117601 (2002).
- [32] Yaroslav Tserkovnyak, Arne Brataas, Gerrit E. W. Bauer, and Bertrand I. Halperin, "Nonlocal magnetization dynamics in ferromagnetic heterostructures," *Reviews of Modern Physics* **77**, 1375–1421 (2005).
- [33] Shigemi Mizukami, Yasuo Ando, and Terunobu Miyazaki, "The study on ferromagnetic resonance linewidth for NM/80NiFe/NM (NM=Cu, Ta, Pd and Pt) films," *Japanese Journal of Applied Physics* **40**, 580–585 (2001).
- [34] J. Foros, G. Woltersdorf, B. Heinrich, and A. Brataas, "Scattering of spin current injected in Pd(001)," *Journal of Applied Physics* **97**, 10A714 (2005).
- [35] J. Nogués and Ivan K Schuller, "Exchange bias," *Journal of Magnetism and Magnetic Materials* **192**, 203–232 (1999).
- [36] R. Jungblut, R. Coehoorn, M. T. Johnson, J. aan de Stegge, and A. Reinders, "Orientational dependence of the exchange biasing in molecular-beam-epitaxy-grown $\text{Ni}_{80}\text{Fe}_{20}/\text{Fe}_{50}\text{Mn}_{50}$ bilayers," *Journal of Applied Physics* **75**, 6659–6664 (1994).
- [37] Jack Bass and William P Pratt, "Spin-diffusion lengths in metals and alloys, and spin-flipping at metal/metal interfaces: an experimentalist's critical review," *Journal of Physics: Condensed Matter* **19**, 183201 (2007).
- [38] Freeman J. Dyson, "Electron spin resonance absorption in metals. II. theory of electron diffusion and the skin effect," *Physical Review* **98**, 349–359 (1955).
- [39] See Supplemental Material [URL will be inserted by publisher] for additional FMR data and their analysis, as well as the modeling of the exchange bias in the AF/Fs bilayer as a function of temperature.
- [40] A. F. Kravets, D. M. Polishchuk, Yu. I. Dzhezheriya, A. I. Tovstolytkin, V. O. Golub, and V. Korenivski, "Anisotropic magnetization relaxation in ferromagnetic multilayers with variable interlayer exchange coupling," *Physical Review B* **94**, 064429 (2016).
- [41] A. P. Malozemoff, "Random-field model of exchange anisotropy at rough ferromagnetic-antiferromagnetic interfaces," *Physical Review B* **35**, 3679–3682 (1987).
- [42] D. Mauri, H. C. Siegmann, P. S. Bagus, and E. Kay, "Simple model for thin ferromagnetic films exchange coupled to an antiferromagnetic substrate," *Journal of Applied Physics* **62**, 3047–3049 (1987).
- [43] W. J. Antel, F. Perjeru, and G. R. Harp, "Spin structure at the interface of exchange biased FeMn/Co bilayers," *Physical Review Letters* **83**, 1439–1442 (1999).
- [44] Yaroslav Tserkovnyak, Arne Brataas, and Gerrit E. W. Bauer, "Dynamic stiffness of spin valves," *Physical Review B* **67**, 140404(R) (2003).
- [45] Tomohiro Taniguchi and Hiroshi Imamura, "Enhancement of the gilbert damping constant due to spin pumping in noncollinear ferromagnet/nonmagnet/ferromagnet trilayer systems," *Physical Review B* **76**, 092402 (2007).

SUPPLEMENTAL MATERIAL

NOTE 1. Resonance field of the free Py(8) layer as a function of temperature

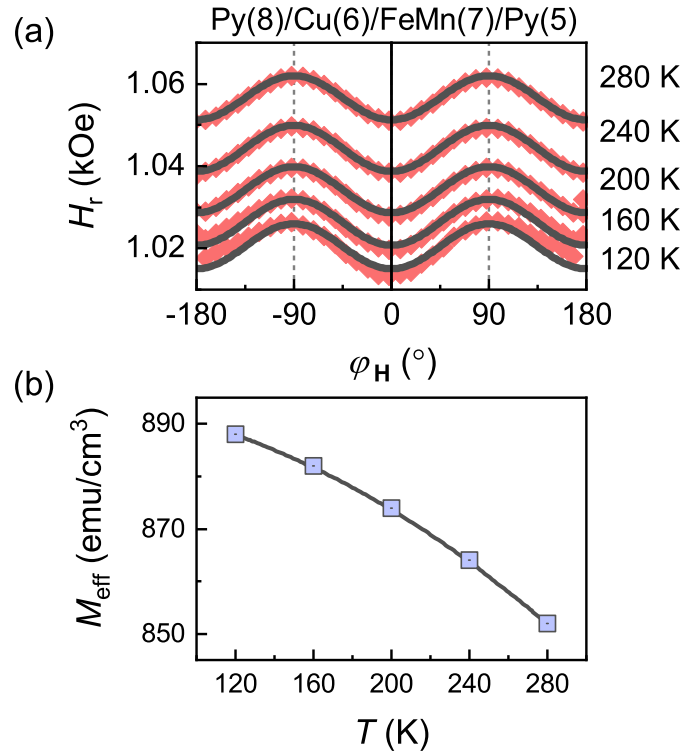


Figure A1. (a) Resonance field of the free Py(8) layer as a function of temperature. (a) In-plane angular profile of the resonance field (H_r) shows the same weak uniaxial magnetic anisotropy at all temperatures. The slight increase in the magnitude of H_r is due to the thermal demagnetization (decrease in the effective magnetization, M_{eff}) of the free Py layer, shown in panel (b). The values of M_{eff} at the given measurement temperatures were obtained from fitting the H_r -vs- φ_H profiles [solid lines in panel (a)] using the standard FMR phenomenology [J. Smit and H. G. Beljers, Phillips Res. Rep. 10, 113 (1955)].

NOTE 2. Resonance field and FMR linewidth versus temperature

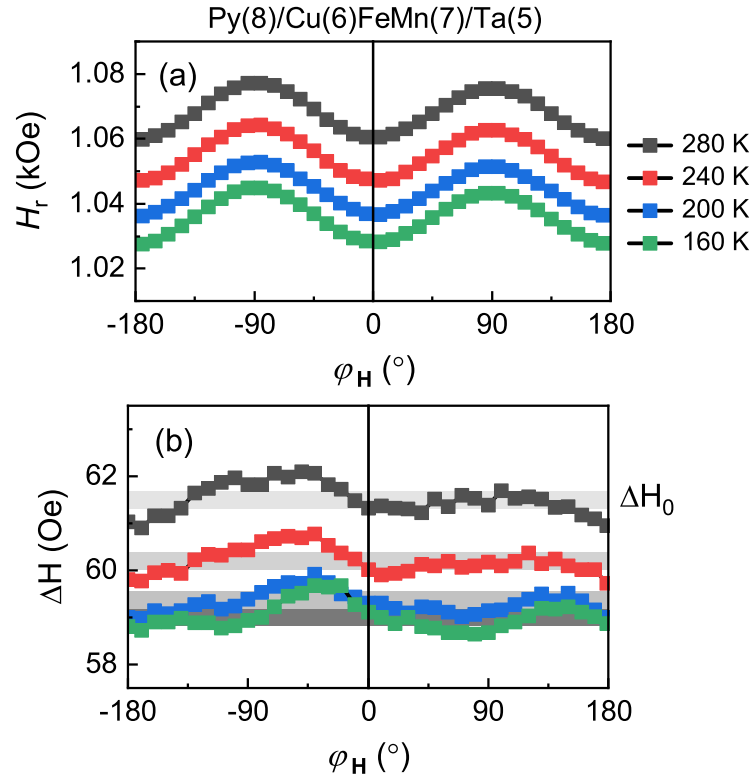


Figure A2. Resonance field and FMR linewidth versus temperature for the structure with a nonmagnetic seed layer (with FeMn/Ta bilayer). (a) In-plane angular profiles of the resonance field of the free Py layer show a similar behavior to that for the structure with a magnetic seed layer [with FeMn/Py bilayer; see Fig. A1(a)]. (b) FMR linewidth (ΔH) shows a much less pronounced angular dependence at all temperatures, which is in contrast to the significant temperature induced changes in ΔH for the structure with FeMn/Py [Figs. 2(c), 3(a)].

NOTE 3. Rotation of the Néel vector of the AF

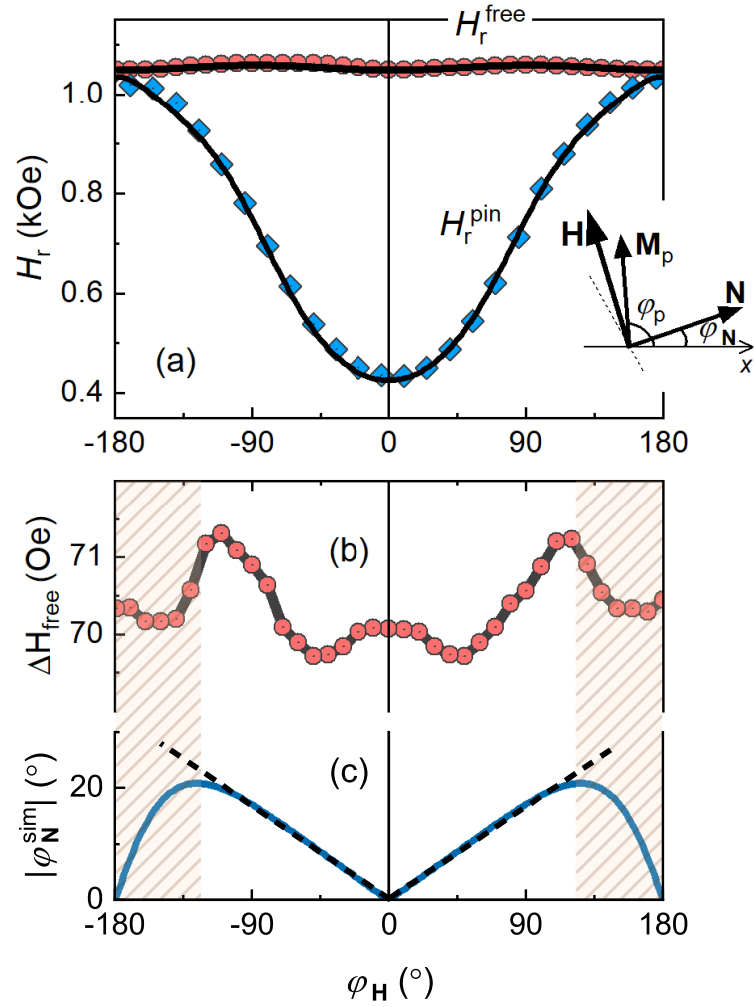


Figure A3. Rotation of the Néel vector of the AF extracted from the angular dependences of the resonance field using the model fit detailed in Note 1. (a) In-plane angular dependences of the resonance field for the free Py layer (H_r^{free}) and the pinned Py layer (H_r^{pin}) of the Py(8)/Cu(5)/FeMn(5)/Py(5) structure, measured at 280 K. The lines are the fits performed using the model of Note 4. (b) Corresponding angular dependences of the FMR linewidth of the free Py layer (ΔH_{free}) and (c) simulated misalignment of the Néel vector (φ_N^{sim}) relative to the exchange-pinning direction ($\varphi_H = 0^\circ$) set at fabrication in the FeMn/Py bilayer. The dependence in (c) was calculated using the parameters obtained from the model fit shown in (a).

The misalignment φ_N^{sim} is linear in φ_H in the angle interval between the two maxima in ΔH_{free} -vs- φ_H , shown in (b).

NOTE 4. Gibbs free energy for F/AF bilayers

To model the deviation of the Néel vector of the F/AF bilayer from its easy (exchange-pinning) direction, we split the energy term commonly used for describing exchange bias into two terms, corresponding to the interlayer exchange coupling at the F/AF interface and the magnetic anisotropy in AF. The Gibbs free energy per unit volume becomes where J_F and J_{AF} are the constants of the uniaxial magnetic anisotropy in the pinned ferromagnetic Py and the antiferromagnetic FeMn layers, respectively; J_{ex} is the constant of exchange coupling at the Py/FeMn interface; Z and G_{dem} are the Zeeman and demagnetization energies; \mathbf{m}_p is the unit vector along magnetization \mathbf{M}_p of the pinned Py.

$$\begin{aligned} G_p &= Z + G_F + G_{AF} + G_{ex} + G_{dem} = \\ &= -\mathbf{M}_p \mathbf{H} - J_F (\mathbf{x} \cdot \mathbf{m}_p)^2 - J_{AF} (\mathbf{x} \cdot \mathbf{N})^2 - J_{ex} (\mathbf{m}_p \cdot \mathbf{N}) + 2\pi M_p^2 (\mathbf{z} \cdot \mathbf{m}_p)^2. \end{aligned} \quad (A1)$$

When external magnetic field \mathbf{H} is oriented in the film plane, terms G_F , G_{AF} , and G_{ex} can be transformed as follows: $G_F = -0.5M_p H_{ua} \cos 2\varphi_p$, $G_{AF} = -J_{AF} \cos \varphi_N$ and $G_{ex} = -M_p H_{ex} \cos(\varphi_p - \varphi_N)$, where angles φ_p and φ_N are defined in the inset to Fig. A3(a). Minimization of (A1) gives

$$\begin{cases} \frac{J_{AF}}{J_{ex}} \sin(2\varphi_N) = \sin(\varphi_p - \varphi_N), \\ \frac{Z}{J_{ex}} \sin(\varphi_p - \varphi_H) = -\sin(\varphi_p - \varphi_N), \end{cases} \quad (A2)$$

where $Z = HM_p$.

Equations (A1) and (A2) can be used for fitting the angular dependence of the FMR spectra of the pinned Py layer in the general case of non-rigid \mathbf{N} . Curve $H_r^{pin}(\varphi_H)$ in Fig. A3(a) is an example of such fitting, showing a good agreement between the fit and the experimental data.